Temperature-Responsive Permeability of Porous PNIPAAm-*g*-PE Membranes

TAO PENG, YU-LING CHENG

Department of Chemical Engineering and Applied Chemistry, University of Toronto, Toronto M5S 3E5, Canada

Received 12 January 1998; accepted 14 March 1998

ABSTRACT: Grafting a temperature-responsive polymer, poly(*N*-isopropylacrylamide) (PNIPAAm), onto porous polyethylene (PE) membranes by UV irradiation was investigated. A wide range of graft yields (5–449%) was achieved by varying irradiation time (20–240 min) and monomer concentration (1.2–3.6 wt %). Characterization by XPS and SEM shows that the graft polymers are located both on the external surfaces as well as inside the pores of the membranes. Diffusional permeation experiments show that two distinct types of temperature responses were observed, depending on the graft yield; permeability increases with temperature in low graft yield membranes, while permeability decreases with temperature in high graft yield membranes. A mechanism explaining the dual valve functions of the graft membrane is proposed based on the location of the graft polymers on the membrane. It was also observed the permeability response exhibits a maximum with permeant molecular weight. © 1998 John Wiley & Sons, Inc. J Appl Polym Sci 70: 2133–2142, 1998

Key words: responsive membranes; grafted polymers; permeability response

INTRODUCTION

Polymeric membranes whose permeability can be changed in response to environmental stimuli such as temperature, pH, light, electric field, and chemical or biological species have been widely studied.[1–14] These environment responsive membranes may find applications ranging from controlled drug delivery[15,16] to chemical separation,[1,17] to tissue engineering.[18] Various types of membranes have been investigated, including homogeneous[1] and heterogeneous[6] hydrogels, membranes that contain liquid crystalline regions[9] or conductive polymers,[10] and porous membranes with grafted or adsorbed responsive polymer chains.[2–5,7,8,11–14]

One type of responsive membranes is prepared by grafting responsive polymers onto porous membrane substrates via various techniques.[2–5, 7,11–14] An advantage of such a membrane is that the porous substrate acts as a dimensionally stable matrix for mechanical support, while the conformational changes of the graft polymer induced by environmental stimuli lead to permeability changes. In addition, the permeability response of this type of membranes may be faster than their corresponding homogeneous analogs. Because grafted chains should have freely mobile ends, distinct from the typical crosslinked network structure in hydrogels that gives rise to relatively immobile chain ends, more rapid conformational changes are expected.[19,20]

Temperature-, pH- or photosensitive polymers have been grafted onto porous substrates.[2–5,7,11–14] The grafted polymers may be located mainly on the external membrane surface,[2,12] or they may be on the external surface as well as inside the pores,[4,7,14] depending on the grafting conditions. For example, in some reports of plasma-induced graft polymerization, active species for initiating are generated mainly near the membrane sur-

Correspondence to: Y.-L. Cheng (ylc@chem-eng.utoronto.ca).

Journal of Applied Polymer Science, Vol. 70, 2133–2142 (1998)
 CCC 0021-8995/98/112133-10

face, resulting in preferential surface grafting.[2,12] Globally grafted membranes are expected to exhibit more pronounced response than those with primarily surface grafts.[21]

Studies on hydraulic permeability (i.e., pressure-driven convective flow of solvents) and diffusional permeability (concentration-driven molecular diffusion of solutes) have been conducted on temperature-, pH- or photosensitive polymers. For some applications, such as drug delivery, mass transport usually occurs via diffusion. It has been experimentally observed that the hydraulic permeability of a poly(acrylic acid)-grafted porous poly(vinylidene fluoride) membrane changed by three orders of magnitude with pH, while the diffusional permeability changed by only a factor of 2.4.[4] Conformation changes of the graft polymer could have a stronger effect on hydraulic permeability because flow rate is proportional to the fourth power of the pore radius,[13] while diffusional rate is only proportional to the square of pore radius.[15]

Some theoretical studies on ionizable polymer brushes have been conducted to correlate properties of the graft polymer chain, for example, brush height and degree of ionization, with the pH and ionic strength of the surrounding solution.[22,23] It was predicted that graft polymer chains would be more effective at controlling the diffusion of long or bulky molecules than that of small species.[23] It was also predicted that the initial membrane pore size and the spacing between grafted chains would have a significant effect on the behavior of the resultant membrane. If pore size and graft spacing were comparable, the collapsed graft polymers would inhibit molecular diffusion through the membrane. In contrast, if the pore size was larger than the graft spacing, grafts would collapse near the pore walls, resulting in the opening of membrane pores and increased diffusional permeability.[23] Thus, the pH dependence of the valve behavior could be tailored by varying the initial pore size of a porous membrane and graft spacing of the resultant membrane. An atomic force microscopy study recently reported the direct visualization of the channel gating process.[24]

Ito et al. investigated the effect of chain length and density of grafted polymers on the pH-dependent hydraulic permeability of poly(acrylic acid)-grafted straight-pored polycarbonate membrane.[25] It was concluded that permeability response was most marked in membranes with intermediate graft density and degree of polymerization. In another study with poly(acrylic acid)-grafted porous cellulose membranes with averaged pore size of 0.2 μm, these same researchers found that diffusional response was larger in membranes with higher graft yields.[26] The effect of graft yield on permeability response from these two studies appears to be in conflict. However, the different grafting methods and substrates used in the two studies may affect graft location and yield and make it difficult to compare the findings.

Hautojaru et al.[4] found that the pH response in diffusional permeability decreased with increasing graft yield (0 to 93%) for poly(vinylidene fluoride) membranes with a 5-μm pore size grafted with poly(acrylic acid) by the electron beam irradiation method. More recently, Lee et al. found the largest pH sensitivity in membranes with the lowest graft yield. The membrane is also made of poly(vinylidene fluoride) substrate, but with smaller pore size of 0.22 μm with a plasma-induced surface graft of poly(acrylic acid).[27]

Okahata et al. developed pH- and temperature-responsive polymer-grafted porous nylon capsule membranes with large diffusional permeability changes (up to a factor of 225).[3,28] They reported that the permeability response was not affected by graft yield ranging from 35 to 275% when hydrophobic poly(4-vinyl pyridine) was grafted. In contrast, when the graft polymer was relatively hydrophilic, the pH response decreased with increasing graft yield. This trend was observed for poly(acrylic acid) with graft yield ranging from 15 to 100%, and poly(methacrylic acid) with graft yield of 30 to 385%. Moreover, they found that diffusional permeability was higher with the graft polymer in the ionized and swollen form opposite to what other researchers have reported. The authors attributed this valve behavior to the chain length of graft polymers and membrane pore size.[28] The contracted graft polymers covered the inner small pores (1 to 2 nm) of the capsule membrane instead of opening the pores, while, in the swollen state, the expanded graft chains extended out from the membrane surface leading to a pathway for permeation.

The above discussion demonstrates that graft parameters have a strong effect on both hydraulic and diffusional permeability response of responsive polymer-grafted porous membranes. However, different or even conflicting results have been reported. This may be because of discrepancies in substrate membrane properties (e.g., hydrophobic vs. hydrophilic, initial pore size of the membrane ranging from 1 nm to 5 μm) and graft parameters (e.g., graft location, graft yield with different range,

graft methods), which make it difficult to compare the reported results. Ito et al. demonstrated that the magnitude of pH or ionic strength-induced permeability response through benzyl glutamate *N*-carboxanhydride grafted poly(tetrafluoroethylene) membranes depends on graft density and chain length.[29] More such systematic studies are needed to reconcile conflicting reports in the literature.

In addition to the graft density and the initial pore size, permeability response also depends on the solute size. It was found that as polyoxylethylene solute size increased from molecular weight of 1000 to 20,000, the pH-dependent permeabilities response of poly(acrylic acid) grafted porous cellulose membranes increased. [26]

Graft polymerization of vinyl monomers onto polyethylene has been examined in various systems initiated by peroxides, γ-radiation, plasma, electron beam irradiation, and photochemical method.[30–34] The photochemical method is relatively simple and practical compared to other initiation methods. High graft yields have been reported for many vinyl monomers including NIPAAm through photoinduced grafting.[21] Moreover, photochemical initiation may cause grafting to occur both on the surface and throughout the entire thickness of the membrane substrate; this could give rise to larger environmental response compared to membranes with primarily surface grafts.

We are investigating temperature- and pH-sensitive polymer-grafted porous membranes in order to understand the effects of graft yield, molecular size of permeants, initial membrane pore size, and properties of graft polymers on temperature and pH-induced permeability changes. In this article, PNIPAAm-*g*-PE porous membranes with a wide range of graft yield were prepared by UV irradiation. The temperature-dependent permeability response of the grafted membranes was investigated as a function of graft yield and permeant molecular weight.

EXPERIMENTAL

Materials

Low-density polyethylene (LDPE) porous membranes produced by thermally induced phase separation were a gift from 3M Company. The PE membrane is a flat sheet with a 50.5-μm thickness, 70.5% porosity, and an average pore diameter of 0.19 μm as specified by the manufacturer.

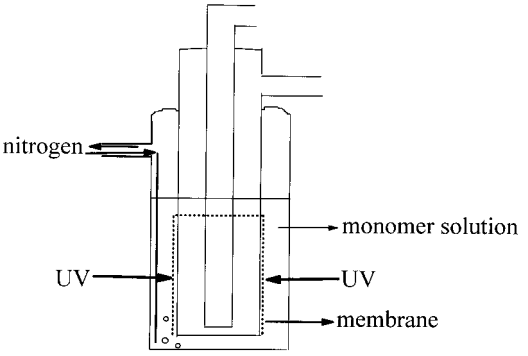

Figure 1 UV reactor of graft polymerization.

N-Isopropylacrylamide (NIPAAm) monomer and photoinitiator xanthone were purchased from Aldrich Co. and used as received.

Graft Polymerization

The PE substrate membrane was cut into 7 $\times$ 10.5 cm rectangular pieces, washed by acetone extraction for 24 h, vacuum dried at room temperature, and weighed. The membrane was then soaked in acetone solution containing 0.3 wt % xanthone for 24 h, removed from solution, and dried under vacuum at room temperature to prepare a xanthone-adsorbed film. Because the pores of the substrate are readily wetted by acetone, it is expected that xanthone should distribute throughout the entire film thickness.

The apparatus shown in Figure 1 was used for the graft polymerization reaction. Aqueous NIPAAm solution (135 mL) of known concentration ranging between 1.2 and 3.6 wt % was introduced into the reactor and purged with nitrogen for 20 min. The xanthone-adsorbed polyethylene film fixed on the surface of the reactor's inner tube was then immersed in the monomer solution. The graft polymerization was initiated by UV irradiation provided by four 300-nm ultraviolet lamps (3.9 watts each) and four 350-nm ultraviolet lamps (4.5 watts each), mounted alternately in a Rayonet photochemical minireactor Model RMR-600 (Southern New England Ultraviolet, Branford, CT). Reaction then proceeded under nitrogen atmosphere for specified amounts of time ranging from 20 to 240 min. The reacted membrane was washed with 2 L deionized water at room temperature for at least 24 h, while the water was changed every 8 h. The membrane was then dried under vacuum. The washing procedure was repeated until a stable dry membrane weight was obtained. Graft yield was then calculated as

$(W_t\text{-}W_o)/W_o$, where W_o and W_t are the dry weights of the membrane before and after grafting, respectively.

Characterization: XPS and SEM

Graft membranes were analyzed with an X-ray photoelectron spectrometer (XPS, Max 200) with a Mg Kα X-ray radiation source at a pressure of 10^{-5} Nm^{-2} and an electron takeoff angle of 90°. The binding energies of the electrons were referenced to carbon at 285 eV. Surface atomic ratios were calculated from peak areas using sensitivity factors for the instrument configuration.

The morphology of the membrane cross sections was visualized by a scanning electron microscope (Hitachi S2500). The samples were first freeze fractured under liquid nitrogen and mounted on a SEM stub with glue. Carbon paint was used to connect the samples with the stub. All the samples were then vapor coated with gold in a sputter coating system.

Permeability Measurement

Permeation experiments were carried out using standard side by side diffusion cells. The grafted membranes were cut into discs and soaked first in methanol to wet the membrane, then pH 7.4 phosphate buffer with the ionic strength of 0.01 *M*. Each test membrane was immersed in the buffer at the appropriate temperature for more than 12 h prior to initiating permeation experiments. After checking for leakage, 25 mL of pH 7.4 phosphate buffer solution with ionic strength of 0.01 *M*, and permeant solution in the same buffer were added simultaneously to the receptor and acceptor cells, respectively, and stirred with a pair of magnetic bars. At periodic time intervals 0.2 mL of solution was removed from the receptor cell, and solute concentration was determined by UV (Hewlett-Packard 8452Win Diode-array UV spectrophotometer). The sample was replaced with 0.2 mL blank buffer. Permeability was calculated using

$$\ln(1 - 2\ C_r/C_0) = -2\ PA\ t/(LV)$$

where C_r is the concentration in the receptor cell at time t, and C_0, P, A, L, and V are the initial solute concentration in the donor compartment, permeability, effective diffusion area, thickness of the dry membrane, and volume of the receptor compartment. The permeability coefficient P can be calculated from the slope of the straight line obtained by plotting $\ln(1-2Cr/C_o)$ versus t. By using the dry membrane thickness to calculate permeability, the permeability response reported in this article is representative of the ratio of permeation rates for a given membrane at different temperatures.

After the permeation experiment, the membrane was put in the pH 7.4 buffer at the appropriate temperature, and its thickness was measured by a micrometer with accuracy of 0.01 mm. The equilibrium state was reached when there were no thickness changes after 12 h.

Table I Graft Yield of Membranes Prepared by UV Irradiation Under Various Conditions

Monomer Concentration (wt %)	Irradiation Time (min)	Graft Yield (%)
1.2	60	5
2.43	60	153
3.6	60	320
2.43	20	28
2.43	30	88
2.43	45	123
2.43	75	233
2.43	90	257
2.43	120	282
2.43	180	394
2.43	240	449

RESULTS AND DISCUSSION

Photochemical Grafting of NIPAAm onto Porous PE

It was found that NIPAAm was easily grafted onto porous polyolefins, especially LDPE . Table I shows that graft yield increases with increasing monomer concentration and irradiation time. Graft yield increases may be ascribed to either increasing chain length or increasing density of the graft polymer; however, no further characterization was done in this study to distinguish between these two possibilities. PNIPAAm-*g*-PE porous membranes with a wide range of graft yields were prepared by varying graft yield, monomer concentration, and irradiation time, and used in subsequent studies.

Characterization of Graft Location: XPS, SEM, and Thickness Measurements

The membrane surface compositions before and after grafting were analyzed by XPS. Figure 2

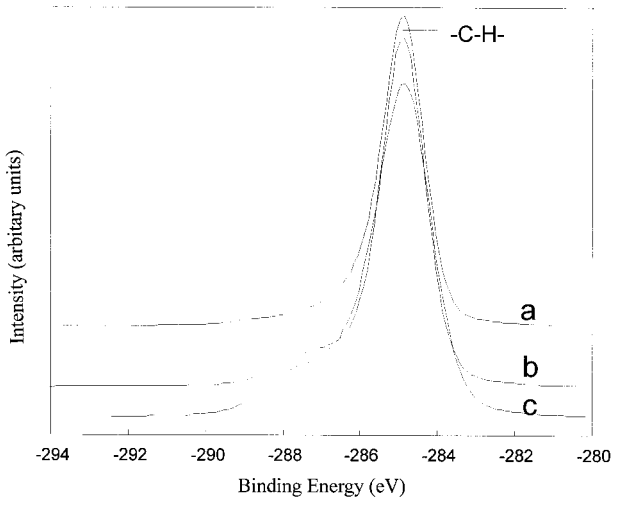

Figure 2 High-resolution XPS scan of C1s peak for the nongraft PE (a) and grafted PE membrane [(b) rear side against the vessel wall; (c) front UV-facing side] with a graft yield of 28%.

shows the high resolution XPS scan of C1s peak for the nascent porous PE membrane [Fig. 2(a)] and the grafted membrane [Fig. 2(b,c)]. For a carbon bonded with electron attractive groups such as the amide group from NIPAAm, a shoulder peak with a higher binding energy would appear beside the normal position at 285.0 eV of the carbon atom in polyethylene.[35] This was observed for both the front UV facing side of the membrane as well as the rear side against the vessel wall. These XPS results are consistent with the presence of PNIPAAm on the membrane surfaces.

The N/C atomic ratios on the surface of membranes with different graft yields were calculated from the sensitivity factor-corrected area under each peak. Figure 3 shows that the ratio increases with increasing graft yield, reaching a plateau of approximately 0.055 at graft yields above about 150%. This can be explained by the grafting process and condition. Our membrane preparation procedure ensures the uniform distribution of photoinitiator throughout the pores at the start of grafting. However, because the pores are not readily wetted by aqueous NIPAAm solutions, little or no monomer is present in the pores at the start of grafting; therefore, surface grafting would predominate at early times, or low graft yields. This would give rise to increasing N/C ratios on the surface at low graft yields. As the surface becomes saturated with PNIPAAm, the surface N/C ratio reaches a plateau.

While surface grafting proceeds, grafted PNIPAAm near the mouth of pores would attract water into the pores, and cause progressively inward wetting of the pores by the NIPAAm solution, thus introducing the monomer into the pores and facilitating grafting inside the pores. Once the pores are wetted, diffusion of NIPAAm into the pores would continually replace the reacted monomer and perpetuate grafting in the pores. Bulk grafting can, therefore, begin well before the surface is covered. Graft yield can continue to increase with little further increase in surface N/C ratio due to increased bulk grafting and/or increased thickness of surface layer beyond the thickness detection limit of XPS. In addition, due to the large pore areas, pore graft can dominate surface graft even at low graft yields (below 150%).

Figure 3 also shows that more polymer was grafted on the front side of the membrane than on the rear side, especially at low graft yield. This can be attributed to the easier access of monomer to the front side of the membrane. At longer grafting times, or higher graft yields, the difference diminishes. The highest surface N/C atomic ratio of 0.06 measured for the membrane with 320% graft yield is lower than the theoretical value for the NIPAAm monomer (0.17). This indicates that the surface was not covered completely by the graft polymer, which is consistent with the SEM results described below.

SEM pictures showing the cross-section morphologies of the nascent PE membrane and grafted membranes are presented in Figure 4. Significantly different structures between nas-

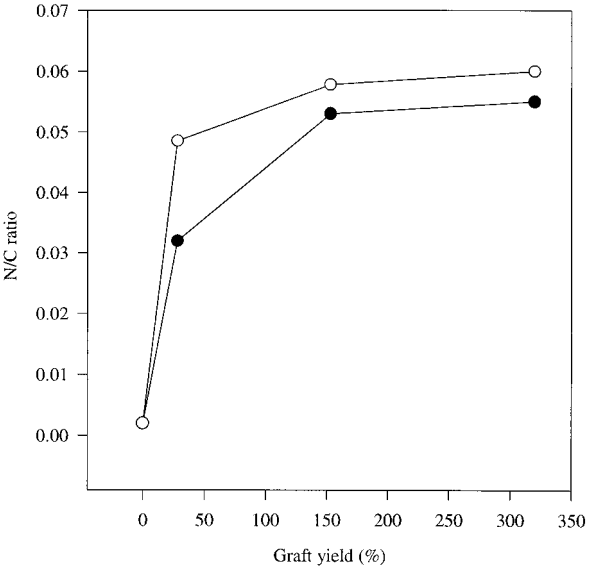

Figure 3 N/C atomic ratios of the surfaces of PNIPAAm-*g*-PE membranes with different graft yields: (○) for front UV-facing side; (●) for rear side against the vessel wall.

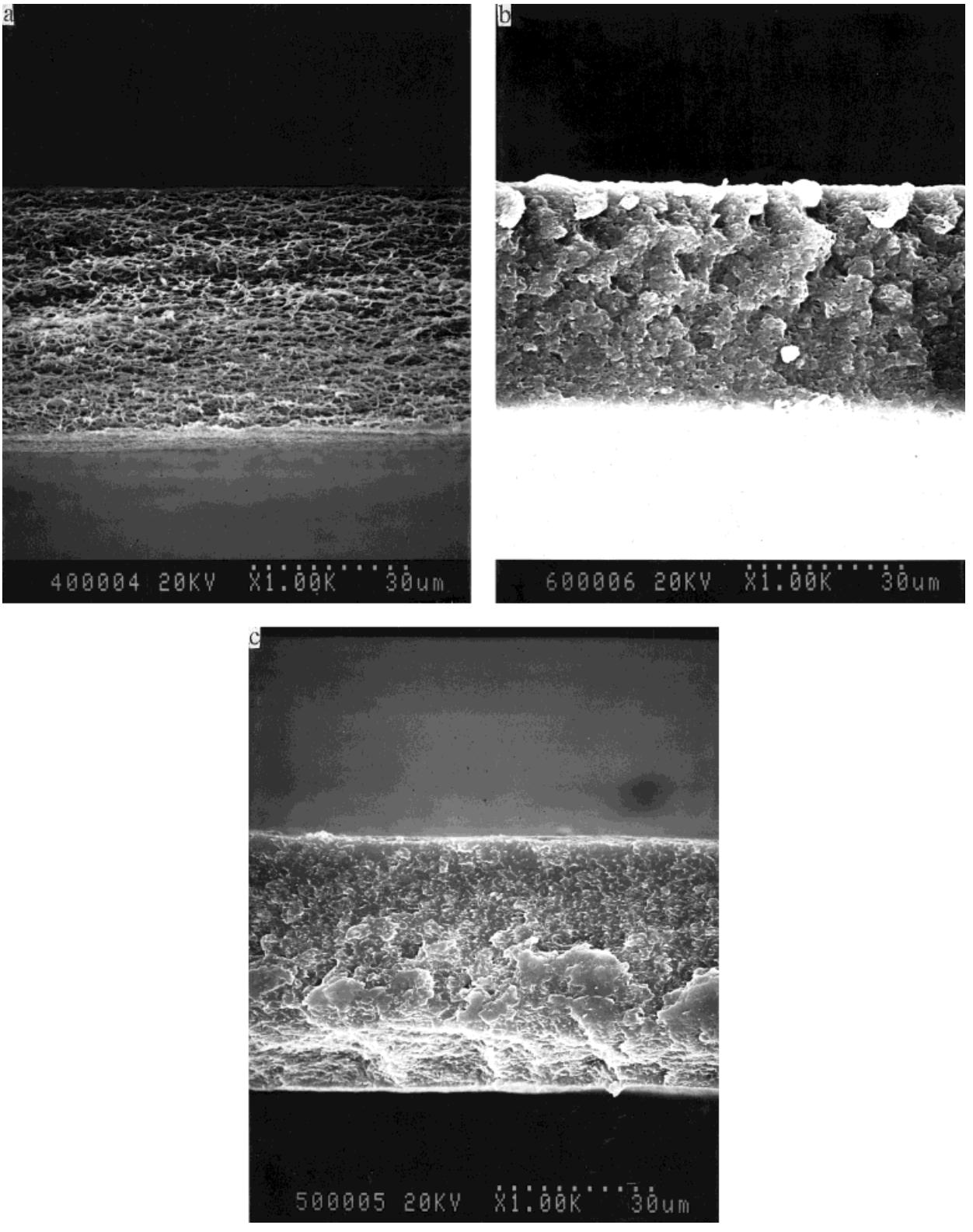

Figure 4 Cross sections of nongrafted (a) and grafted porous PE membranes with graft yields of 233% (b) and 320% (c).

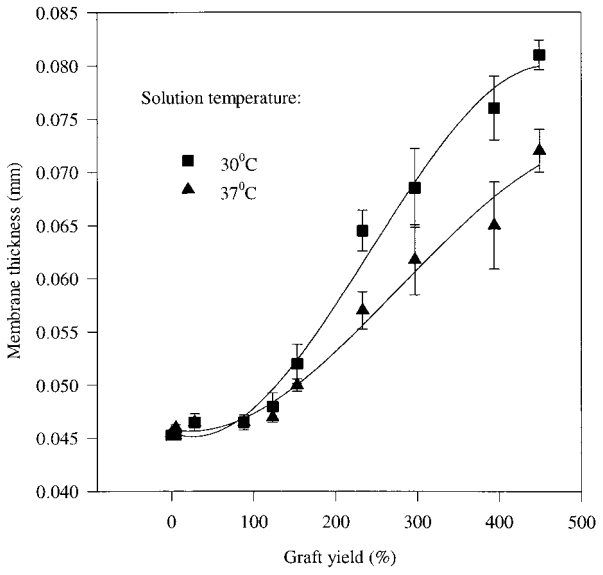

Figure 5 The membrane thickness as a function of the graft yield at the solution tempeature below and above the LCST. Error bars are standard deviation (n = 4).

cent and grafted PE membranes are seen. The fibrils visible in the cross section of the nascent PE membrane are covered by the graft polymers throughout the entire membrane thickness. Coverage appears to be denser in the 320% graft yield membrane than the 233% graft yield membrane.

The thickness of the membrane in pH 7.4 buffer solution at the temperature below and above the lower critical solution temperature (LCST) of PNIPAAm was measured to characterize dimensional changes. Figure 5 shows that membranes with graft yield less than 153% have about the same thickness as the nascent membranes and do not show dimensional changes with temperature. In contrast, at graft yields of above 153%, membranes become thicker than the nascent membrane, and the thickness varies in response to temperature. The results suggest that PNIPAAm at low graft yields has no effect on the dimensional change, while, as the pores become filled with increasing graft yield, grafted polymers would extend out of the membrane pores in the solution. As a result, the PE surface is covered by PNIPAAm resulting in the thickness change in response to the temperature variation.

In summary, XPS and SEM results suggest that PNIPAAm was grafted on the surface and throughout the pores of the PE substrate. The combined observations of the effect of graft yield on thickness and the effect of graft yield on surface N/C ratio suggest that at very low graft yields, the membrane surface becomes saturated in PNIPAAm, although most graft is located inside the pores. At high graft yields, the surface PNIPAAm layer increases in thickness, either due to the elongation of surface graft chains, or the extension of pore graft chains out of the pores. This thickness increase is not accompanied by any observable increase in surface N/C ratio. This can be due to either partial surface coverage or due to the dehydration required for XPS analysis.

Permeation Study

Effect of the Graft Yield

The temperature-dependent permeability of vitamin B_{12} through PNIPAAm-*g*-PE of graft yields 233 and 320% are shown in Figures 6 and 7, respectively. It is interesting to note that temperature has opposite effects on the permeability of the 233 and the 320% graft yield membranes, indicating that two distinct types of valve functions exist, depending on the graft yield. The two types of valve function are further demonstrated in Figure 8, in which the log permeability of vitamin B_{12} at 35 and 30°C is plotted as a function of graft yield. It is seen that at lower graft yields, the permeability at 35°C is higher than that at 30°C.

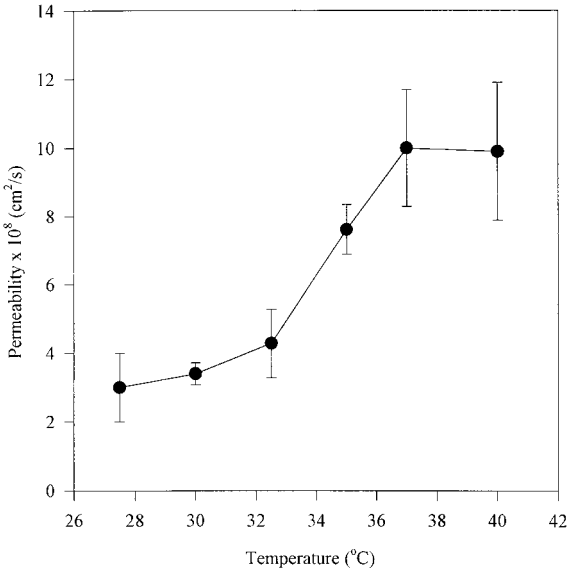

Figure 6 Effect of temperature on the permeability of vitamin B_{12} across a PNIPAAm-*g*-PE porous membrane with graft yield of 233% in pH 7.4 (I = 0.01) buffer solution. Error bars are standard deviation (n = 3).

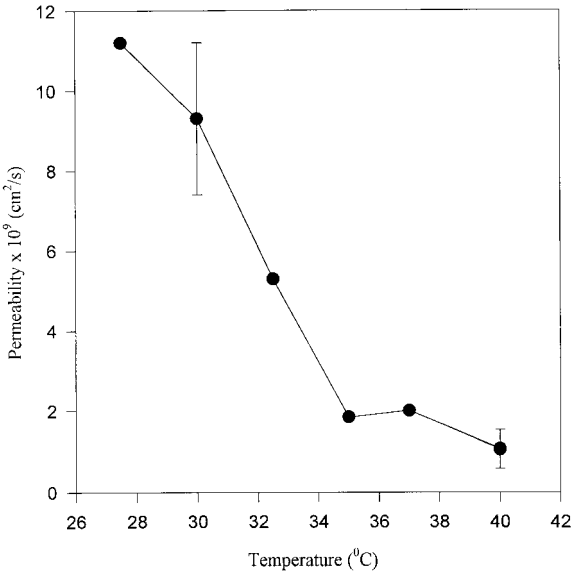

Figure 7 Effect of temperature on the permeation of vitamin B_{12} through a PNIPAAm-*g*-PE porous membrane with a graft yield of 320% in pH 7.4 (I = 0.01) buffer solution. Error bars are standard deviation (n = 3).

The permeability response increases with graft yield and reaches a maximum at a graft yield of 233%. Then at a transitional value of graft yield, the permeability response switches, and a new pattern of valve function is observed. The permeability now becomes lower at 35°C than at 30°C, opposite the behavior seen in lower graft yield membranes. Moreover, the permeability response generated by second type of valve function is larger than that by the first type (a factor of 12 vs. 2.3 between the higher and lower permeabilities) and the permeability decreases with increasing graft yield up to three orders of magnitude within the range of experimental conditions tested.

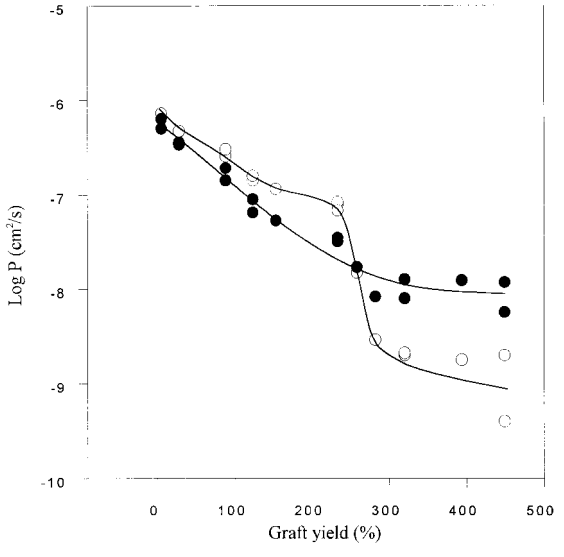

Figure 8 Effect of graft yield on the permeability (P) of vitamin B_{12} across PNIPAAm-*g*-PE porous membranes in pH 7.4 (I = 0.01) buffer solution at 35°C (○) and 30°C (●).

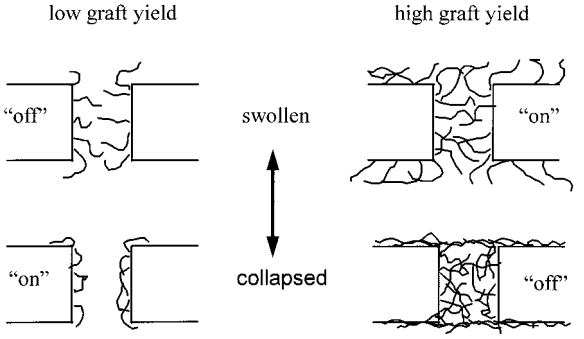

Figure 9 Explanation of the dual-response mechanism.

Thickness measurements (Fig. 5) indicated an increasing surface layer as graft yield increased, implying that as graft yield increases, graft polymer fills the pores and extends out of the pores to form a surface layer of graft polymer. These observations suggest that in the lower graft yield membranes, permeability is controlled by pore-grafted PNIPAAm. The expanded conformation of the grafted polymers below the LCST gives rise to a reduced effective pore size in comparison with the collapsed state above LCST. In the higher graft yield membranes, permeability is controlled by the thick surface layer of PNIPAAm. As the surface PNIPAAm layer shrinks with increasing temperature, the layer becomes more compacted and more resistant to diffusion, resulting in decreased permeability. The permeability response of higher graft yield membranes, i.e., higher permeability below the LCST than above, is consistent with PNIPAAm-based hydrogel membranes.[1] The two response mechanisms are illustrated schematically in Figure 9.

Effect of Permeant Size

Figure 10 shows the effect of solute size on the permeability response of the membrane with graft yield of 233 and 449%. The permeability response is measured as the ratios of permeabilities at 37 and 30°C for 233% graft yield or 30 and

37°C for 449% graft yield, respectively. For both membranes, the responsiveness shows a maximum at an intermediate solute molecular weight.

Figure 11 schematically illustrates a possible explanation for this observation. In the pore-graft controlled low graft yield membrane [Fig. 11(a)], size exclusion occurs when the solute size is within an order or magnitude of the effective pore dimension of the membrane. The effective pore size of the membrane changes due to the swelling or collapse of the graft polymer. The smallest penetrants are not significantly affected by the changing pore size because the effective pore size, even with swollen grafts, is much larger than the penetrant. The largest penentrants are not significantly affected by the changing pore size because the effective pore size, in both the swollen and collapsed states, is comparable to penentrant size, and significant size exclusion exists in both states. For the intermediate sized penetrants, the change in pore size due to graft collapse or swelling represents a significant change in the extent of size exclusion, giving rise to the largest permeability response. A similar explanation can be applied to the higher yield membranes in which surface PNIPAAm layers control the permeability behavior [Fig. 11(b)]. The response behavior is similar to that of PNIPAAm hydrogel membranes, and size exclusion occurs when the solute dimensions approach the effective mesh size within the surface PNIPAAm layer.

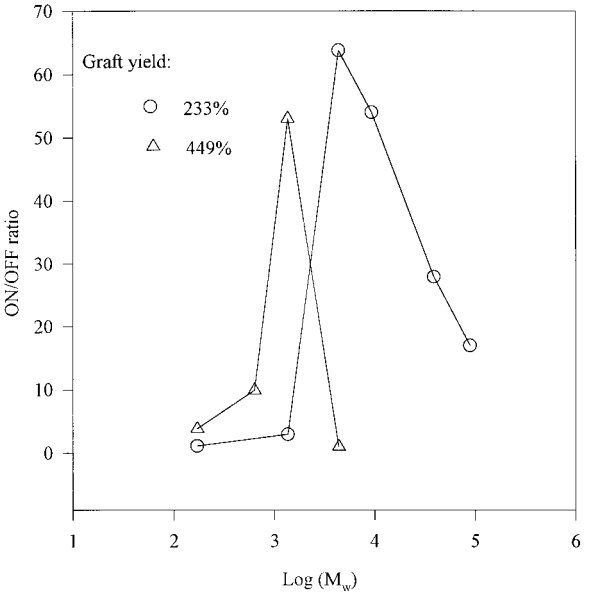

Figure 10 Effect of the molecular weight (M_w) of solutes on the permeability response of the PNIPAAm-*g*-PE membrane.

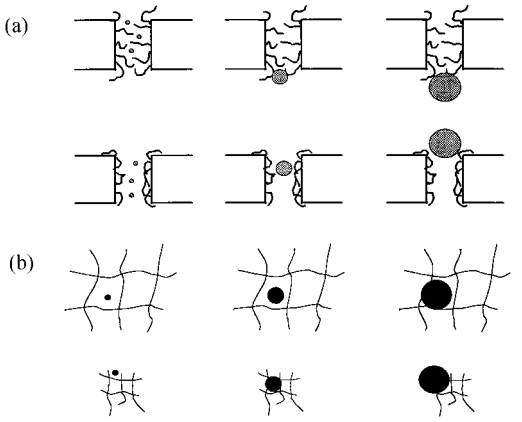

Figure 11 Explanation of the size exclusion effect on the two types of permeability response: (a) polymer-grafted porous membranes with low graft yields; (b) graft layers on the surface of polymer-grafted porous membranes with high graft yields.

CONCLUSIONS

1. Poly(*N*-isopropylacrylamide)-filled porous polyethylene membranes with a wide range of graft yields can be prepared by photochemical graft polymerization. The graft polymer is located on both sides of the external surface and inside the pores of the membrane.
2. PNIPAAm grafts are predominantly located within the pores in low graft yield membranes. These membranes exhibit little change in thickness with solution temperatures, and the membranes permeability increases when temperature increases above the LCST.
3. In high graft yield membranes, the membrane pores are filled with the graft polymer and the membrane surface may be covered by graft layers. As a result, the membrane thickness increases with graft yield and becomes sensitive to solution temperatures. Moreover, the membrane shows abrupt decreased permeabilities as the temperature is raised through the LCST.
4. The permeability response exhibits a maximum at intermediate solute size.

REFERENCES

1. H. Feil, Y. H. Bae, J. Feijen, and S. W. Kim, *J. Membr. Sci.,* **64,** 283 (1991).

2. Y. M. Lee, S. Y. Ihm, J. K. Shim, J. H. Kim, C. S. Cho, and Y. K. Sung, *Polymer,* **36,** 81 (1995).
3. Y. Okakata, Y. Noguchi, and T. Seki, *Macromolecules,* **19,** 493 (1986).
4. J. Hautojarvi, K. Kontturi, J. H. Nasman, B. L. Svarfvar, P. Viinikka, and M. Vuoristo, *Ind. Eng. Chem. Res.,* **35,** 450 (1996).
5. Y. Okahata, H. Noguchi, and T. Seki, *Macromolecules,* **20,** 15 (1987).
6. J. S. A. Turner and Y. L. Cheng, *5th World Biomater. Congress,* 1996, I-878.
7. D. Chung, Y. Ito, and Y. Imanishi, *J. Appl. Polym. Sci.,* **51,** 2027 (1994).
8. M. Sato, T. Kinoshita, A. Takizawa, Y. Tsujita, and Ito R., *Polym. J.,* **20,** 761 (1988).
9. Y. Ly and Y-L. Cheng, *J. Membr. Sci.,* **77,** 99 (1993).
10. L. Stassen, T. Sloboda, and G. Hambitzer, *Synth. Met.,* **71,** 2243 (1995).
11. M. A. Islam, A. Dimov, and A. L. Malinova, *J. Membr. Sci.,* **66,** 69 (1992).
12. H. Iwata and T. Matsuda, *J. Membr. Sci.,* **38,** 185 (1988).
13. S. Cartier, T.A. Horbett, and B. D. Ratner, *J. Membr. Sci.,* **106,** 17 (1995).
14. M. Casolaro and R. Barbucci, *Colloids Surfaces A: Physicochem. Eng. Aspects,* **77,** 81 (1993).
15. C. L. Bell and N. A. Peppas, *Adv. Polym. Sci.,* **122,** 125 (1994).
16. S. H. Gehrke, *Adv. Polym. Sci.,* **110,** 80 (1993).
17. A. J. Grodzinsky and A. M. Weiss, *Separat. Purificat. Methods,* **14,** 1 (1985).
18. B. L. Vernon, S. W. Kim, and Y. H. Bae, *Proceed. 5th World Biomater. Congress,* 1996, I-870.
19. R. Yoshida, K. Uchida, Y. Kaneko, K. Sakai, A. Klkuchi, Y. Sakural, and T. Okano, *Nature,* **374,** 240 (1995).
20. Y. G. Takei, T. Aoki, K. Sanui, N. Ogata, Y. Sakurai, and T. Okano, *Macromolecules,* **27,** 6163 (1994).
21. H. Kubota, N. Nagaoka, R. Katakai, M. Yoshida, H. Omichi, and Y. Hata, *J. Appl. Polym. Sci.,* **51,** 925 (1994).
22. F. von Goeler and M. Muthukumar, *Macromolecules,* **28,** 6608 (1995).
23. R. Israels, D. Gersappe, M. Fasolka, V. A. Roberts, and A. Balazs, *Macromolecules,* **27,** 6679 (1994).
24. Y. Ito, Y. S. Park, and Y. Imanishi, *J. Am. Chem. Soc.,* **119,** 2739 (1997).
25. Y. Ito, S. Kotera, M. Inaba, K. Kono, and Y. Imanishi, *Polymer,* **31,** 2157 (1990).
26. Y. Ito, M. Casolaro, K. Kono, and Y. Imanishi, *J. Control. Rel.,* **10,** 95 (1989).
27. Y. M. Lee and J. K. Shim, *J. Appl. Polym. Sci.,* **61,** 1245 (1996).
28. Y. Okahata, H. Noguchi, and T. Seki, *Macromolecules,* **20,** 15 (1987).
29. Y. Ito, Y. Ochiai, Y. S. Park, and Y. Imanishi, *J. Am. Chem. Soc.,* **119,** 1619 (1997).
30. E. M. Abdel-Bary, A. M. Dessouki, E. M. Elnesr, and A. A. Elmiligy, *Polym.-Plast. Technol. Eng.,* **34,** 383 (1995).
31. M. Suzuki, A. Kishda, H. Iwata, and Y. Ikada, *Macromolecules,* **19,** 1804 (1986).
32. T. Yamaguchi, S. Nakao, and S. Kinura, *Macromolecules,* **24,** 5522 (1991).
33. A. Wirsen, K. T. Lindberg, and A. C. Albertsson, *Polymer,* **37,** 761 (1996).
34. M. Imaizumi, H. Kubota, and Y. Hata, *Eur. Polym. J.,* **30,** 979 (1994).
35. G. Beamson and D. Briggs, *High Resolution XPS of Organic Polymers: The Scienta ESCA300 Database,* John Wiley & Sons Ltd, London, 1992, p. 54.